Cerebral Cortex, November 2021;31: 5056–5066

https://doi.org/10.1093/cercor/bhab141
Advance Access Publication Date: 11 June 2021
Original Article

ORIGINAL ARTICLE

Movement-Related Gamma Synchrony Differentially Predicts Behavior in the Presence of Visual Interference Across the Lifespan

Rachel K. Spooner[1,2], Yasra Arif[1,2], Brittany K. Taylor[1] and Tony W. Wilson[1,2]

[1]Institute for Human Neuroscience, Boys Town National Research Hospital, Omaha, NE 68010, USA and [2]College of Medicine, University of Nebraska Medical Center, Omaha, NE 68198, USA

Address correspondence to Tony W. Wilson, Institute for Human Neuroscience, Boys Town National Research Hospital, Omaha, NE 68010, USA. Email: tony.wilson@boystown.org

Abstract

The ability to allocate neural resources to task-relevant stimuli, while inhibiting distracting information in the surrounding environment (i.e., selective attention) is critical for high-level cognitive function, and declines in this ability have been linked to functional deficits in later life. Studies of age-related declines in selective attention have focused on frontal circuitry, with almost no work evaluating the contribution of motor cortical dynamics to successful task performance. Herein, we examined 69 healthy adults (23–72 years old) who completed a flanker task during magnetoencephalography (MEG). MEG data were imaged in the time-frequency domain using a beamformer to evaluate the contribution of motor cortical dynamics to age-related increases in behavioral interference effects. Our results showed that gamma oscillations in the contralateral motor cortex (M1) were a robust predictor of reaction time, regardless of interference level. Additionally, we observed condition-wise differences in gamma-by-age interactions, such that in younger adults, increases in M1 gamma power were predictive of faster reaction times during incongruent trials, while older adults did not receive this same behavioral benefit. Importantly, these data indicate that M1 gamma oscillations are differentially predictive of behavior in the presence, but not absence of visual interference, resulting in exhausted compensatory strategies with age.

Key words: Eriksen flanker task, magnetoencephalography, motor oscillations, neural inefficiency, selective attention

Introduction

The cognitive aging process is associated with a variety of changes in brain structure and function, often leading to behavioral decline and functional dependence in later life. Among these behavioral changes are those in selective attention function, which is the ability to allocate attentional resources to behaviorally relevant stimuli, while inhibiting distracting information within the surrounding environment (Plude and Doussard-Roosevelt 1989; Hasher et al. 1991; Driver 2001; Carrasco 2011). Importantly, this inhibition of irrelevant or interfering information has been shown to decline steadily across the lifespan (e.g., slower reaction times with increased interference), concomitant with age-related alterations in key attentional hubs, including the frontoparietal network during stimulus processing (Kawai et al. 2012; Geerligs et al. 2014; Langner et al. 2015; Aschenbrenner and Balota 2017; Williams et al. 2018). While the neural mechanisms serving selective attention function have been extensively studied in the context of healthy aging, the contribution of age-related changes in motor control to the declines in behavioral performance seen in visual interference tasks is less well characterized. This is unfortunate, as alterations in the neural dynamics serving motor control may provide key mechanistic insight on the age-related behavioral decline in selective attention, which is a fundamental contributor to a family of functional dependencies observed in later life (Jefferson et al. 2006).

Motor control involves a transformation of desired kinematics into discrete plans to successfully execute motor actions,

often in the presence of environmental distractions. Such motor control requires spatiotemporally precise oscillatory activity during the planning, execution, and termination of motor commands. Briefly, recent neurophysiological studies of movement-related neural oscillations have used magnetoencephalography (MEG), which is a noninvasive imaging method that measures the minute magnetic fields (10^{-15} T) that naturally emanate from active neuronal populations in the brain. Importantly, because magnetic fields are not significantly altered by intervening tissues (e.g., scalp, skull, cerebrospinal fluid), unlike the electrical activity recorded using electroencephalography (EEG), MEG is afforded good spatial precision (~3–5 mm) to accompany its superb temporal resolution (~1 ms), making it an ideal method to quantify the dynamic interactions among spatially- and spectrally-defined neuronal populations (Hämäläinen et al. 1993; Wilson et al. 2016). In regard to motor control, oscillatory power decreases in the alpha (e.g., 10–14 Hz) and beta (e.g., 15–30 Hz) range occur prior to and during movement across an extended motor network, including bilateral primary motor cortices (M1), supplementary motor areas, and superior parietal lobules (Tzagarakis et al. 2010; Wilson et al. 2010, 2014; Grent-'t-Jong et al. 2014; Heinrichs-Graham and Wilson 2015; Heinrichs-Graham et al. 2016). Interestingly, desynchronizations in the alpha and beta frequencies during movement have been closely tied to motor selection and execution processes and likely reflect the active engagement of neuronal pools during these distinct phases of motor control. In contrast, robust increases in beta oscillatory power are observed following motor termination (i.e., postmovement beta rebound, or PMBR) in the M1 contralateral to movement, and are hypothesized to either reflect neuronal populations returning to idling levels, the active inhibition of motor neurons, or sensory reafference to the motor cortex during movement termination (Pfurtscheller and Lopes da Silva 1999; Cassim et al. 2001; Jurkiewicz et al. 2006; Gaetz et al. 2010; Heinrichs-Graham et al. 2017; Wilson et al. 2011). Finally, there are transient increases in low (i.e., theta: 4–8 Hz) and high (i.e., gamma: 60–90 Hz) frequency oscillations that coincide closely with movement onset. While the precise role of movement-related theta and gamma oscillations are less well characterized, recent work suggests that these increases in oscillatory synchrony may serve as temporal coordinators (i.e., theta; Igarashi et al. 2013; Johnson et al. 2017; Tomassini et al. 2017) and execution signals (i.e., gamma; Cheyne et al. 2008; Muthukumaraswamy 2010; Cheyne and Ferrari 2013) for volitional movement in M1.

Interestingly, the spectral composition of movement-related gamma synchrony (MRGS) has been the subject of multiple investigations focused on cognitive processes in recent years (Gaetz et al. 2013; Grent-'t-Jong et al. 2013; Heinrichs-Graham et al. 2018; Spooner, Wiesman, Proskovec, et al. 2020; Wiesman et al. 2020). While MRGS was first proposed as simply an execution signal in the brain, as its spectral properties (e.g., power and/or frequency) are tightly linked to the kinematics of the movement itself (e.g., timing, force applied, muscle groups engaged; Muthukumaraswamy 2010), recent work has shown that it is modulated by higher order cognitive demands, including selective attention and response interference. Essentially, using classic selective attention paradigms such as the Eriksen flanker and multi-source interference tasks, studies have shown that visual interference (i.e., incongruent target stimuli with surrounding distractors) can modulate key parameters of the MRGS (i.e., latency, power, and/or peak frequency) and behavioral task performance (Gaetz et al. 2013; Grent-'t-Jong et al. 2013; Heinrichs-Graham et al. 2018; Wiesman et al. 2020), albeit earlier studies reporting latency differences in the MRGS must be interpreted cautiously, as these effects could reflect prolonged stimulus processing in the presence of interference, rather than differences in motor dynamics directly. Nonetheless, these studies suggest that the spectral and temporal properties of the MRGS may be altered in the presence of visual interference, although their direct impact on the age-related decline in selective attention performance remains unknown and identifying this impact is critical to understanding key attributes of aging. In addition, it is unclear the extent to which MRGS modulates behavioral performance above and beyond other oscillatory signatures of motor control (i.e., perimovement theta, alpha, and beta activity), as prior work has solely characterized changes in these spectral profiles in isolation of one another. Thus, in the current study, we used advanced multiple moderation analyses to test the hypothesis that movement-related gamma oscillations may have a direct role in the age-related decline observed for selective attention processes, such that elevations in gamma power would predict behavioral performance in the presence of interference (i.e., incongruent trials) to a greater extent than other perimovement oscillations in the contralateral M1. Further, we expected this neural mechanism to be exacerbated by the aging process. To examine this, adults aged 23–72 years old completed an arrow-based version of the Eriksen flanker task (Eriksen and Eriksen 1974) during MEG. Advanced oscillatory analyses were applied to the MEG signals to evaluate the contribution of movement-related neural dynamics to the decline in behavioral performance observed in the presence of interference across the lifespan. Importantly, our results suggest that MRGS power in the M1 cortices during motor execution predicts behavioral performance above and beyond other oscillatory signatures of movement and, further, changes in MRGS as a function of age differentially predict task performance in the presence, but not absence of visual interference.

Materials and Methods

Participants

Seventy-two healthy adults (M_{age} = 45.4 years old, SD = 14.92 years, range: 23–72 years old, 33 females) were enrolled in this study. Exclusionary criteria included any medical illness affecting central nervous system function, any neurological or psychiatric disorder, history of head trauma, current pregnancy, current substance use, implanted ferromagnetic objects or extensive dental work, and cognitive impairment. Cognitive impairment was based on a thorough neuropsychological battery that assessed functionality across six domains (i.e., learning, memory, executive function, processing speed, attention, motor function). Participants who scored less than one standard deviation from the mean across two or more cognitive domains using demographically normed scores per test were deemed cognitively impaired and excluded from the study. This resulted in the exclusion of three participants. The battery included the following tests for each domain: "learning" (Hopkins Verbal Learning Test—Revised (HVLT-R) Learning Trials 1–3; Benedict et al. 1998), "memory" (HVLT-R Delayed Recall and Recognition Discriminability Index; Benedict et al. 1998), "executive function" (Comalli Stroop Test Interference Trial; Comalli et al. 1962), semantic verbal fluency (Heaton et al. 2004), phonemic verbal fluency (Heaton et al. 2004), and Trail Making

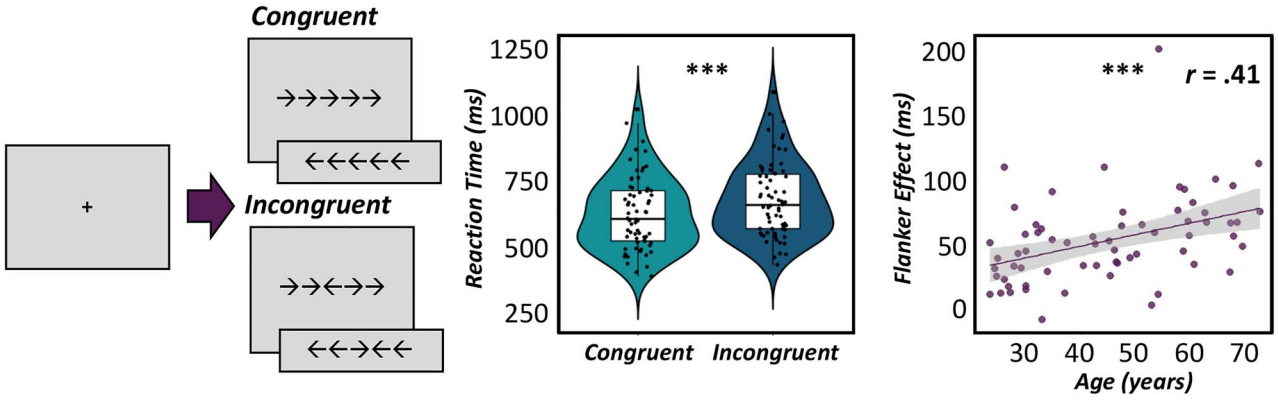

Figure 1. Response interference task and behavior. (Left) Participants completed an arrow-based Eriksen flanker task during MEG. A fixation cross was presented for 1500 ms (±50 ms) followed by the target stimulus consisting of five arrows which was presented for 2500 ms. Participants were instructed to respond to the direction of the middle arrow with their right index (left arrow) or middle finger (right arrow). Stimuli could either be congruent, such that surrounding arrows were pointing in the same direction as the middle arrow; or incongruent, such that the surrounding arrows were pointing in the opposite direction as the middle arrow. Trials were pseudorandomized with equal numbers of each condition (100 trials each) and left and right pointing arrows equally represented throughout. (Middle) Violin and embedded box plots denote reaction time for congruent (light blue) and incongruent (dark blue) trials. Performance on the flanker task showed a significant interference effect across all participants, such that participants were slower to respond to incongruent trials compared with congruent ones. (Right) The scatterplot denotes the positive association between chronological age (in years) on the *x*-axis and reaction time interference effect (incongruent—congruent; in ms) depicted on the *y*-axis. 95% confidence intervals (gray) surround the regression line (in purple). $^{***}P < 0.001$.

Test Part B (Heaton et al. 2004), "processing speed" (Comalli Stroop Test Color Trial; Comalli et al. 1962), Wechsler Adult Intelligence Scale (WAIS-III) Digit Symbol Coding (Wechsler 1997), and Trail Making Part A (Heaton et al. 2004), "attention" (WAIS-III Symbol Search; Heaton et al. 2004), and Comalli Stroop Word Trial (Comalli et al. 1962), and "motor function" (Grooved Pegboard, Dominant and Non-Dominant Hands; Klove 1963). Z-scores were computed using raw scores and composite domain-specific scores were calculated by averaging the Z-scores of assessments that comprised each respective domain (see above). The 69 participants included in the current study had the following domain-specific performance metrics (z-scores mean ± SD): learning (−0.15 ± 1.04), memory (0.03 ± 0.80), executive function (0.18 ± 0.69), processing speed (0.37 ± 0.57), attention (0.47 ± 0.63), and motor function (−0.17 ± 0.78). The University of Nebraska Medical Center Institutional Review Board approved the study and all participants provided written informed consent.

Experimental Paradigm

Participants completed a modified Eriksen flanker task (Eriksen and Eriksen 1974) while seated in a nonmagnetic chair with their head positioned within the MEG helmet-shaped sensor array (Fig. 1). Participants were first presented with a fixation cross for 1500 ms (±50 ms), followed by the target stimulus presented for 2500 ms. The target stimulus consisted of five centrally presented arrows and participants were instructed to respond to the direction of the middle arrow with their right index (left arrow) and middle fingers (right arrow). In congruent trials, all surrounding arrows were pointing in the same direction as the middle arrow, while in incongruent trials, the surrounding arrows were pointing in the opposite direction as the middle arrow. A total of 200 trials (100 trials of each condition) were performed, making the overall MEG recording approximately 14 min in duration. Importantly, trial order was pseudorandomized, with equal representations of left and right pointing arrows presented in each condition.

MEG Data Acquisition and Coregistration with Structural MRI

All recordings were performed in a one-layer magnetically shielded room with active shielding engaged for environmental noise compensation. With an acquisition bandwidth of 0.1–330 Hz, neuromagnetic responses were sampled continuously at 1 kHz using an Elekta/MEGIN MEG system (Helsinki, Finland) with 306 magnetic sensors, including 204 planar gradiometers and 102 magnetometers. Throughout data acquisition, participants were monitored using a real-time audio–video feed from inside the magnetically shielded room. MEG data from each participant were individually corrected for head motion and subjected to noise reduction using the signal space separation method with a temporal extension (Taulu and Simola 2006). Each participant's MEG data were coregistered with their structural T1-weighted MRI data prior to imaging analyses using Brain Electrical Source Analysis (BESA) MRI (Version 2.0). Structural MRI data were aligned parallel to the anterior and posterior commissures and transformed into standardized space. After beamformer analysis (see below), each subject's functional images were transformed into standardized space using the transform that was applied to the structural MRI volume and spatially resampled.

MEG Preprocessing and Sensor-Level Statistics

Cardiac and ocular artifacts were removed from the data using signal-space projection (SSP) and the projection operator was accounted for during source reconstruction (Uusitalo and Ilmoniemi 1997). Epochs were of 4000 ms duration (−2000 to 2000 ms), with 0 ms defined as movement onset and the baseline being the −1800 to −1000 ms window. Epochs containing artifacts were rejected based on an individualized fixed threshold method, which was supplemented with visual inspection. Note that we used individualized thresholds because factors such as head size and proximity to the sensor array can make the absolute amplitude of MEG signals vary significantly across participants. On average, an amplitude threshold of

1045.45 ± 211.90 fT and a gradient threshold of 295.08 ± 128.45 fT/s was used per participant. After artifact rejection, an average of 89.2 ± 7.7 congruent and 88.8 ± 8.2 incongruent trials remained per participant and these were used for further analysis. Importantly, the amount of artifact-free trials did not differ as a function of condition ($P = 0.348$).

Artifact-free epochs were transformed into the time-frequency domain using complex demodulation (Kovach and Gander 2016), and the resulting spectral power estimations per sensor were averaged over trials to generate time-frequency plots of mean spectral density. The sensor-level data per time-frequency bin were normalized using the mean power per frequency during the −1800 to −1000 ms baseline period. The specific time-frequency windows used for imaging were determined by statistical analysis of the sensor-level spectrograms across all participants and trials using a two-stage paired-sample *t*-test against baseline followed by cluster-based permutation testing procedure (initial threshold: $P < 0.05$, permutations: 10 000) to reduce the risk of false positives. First, paired-sample *t*-tests against baseline were conducted on each data point, with the output spectrogram of *t*-values being initially thresholded at $P < 0.05$. Next, time-frequency bins that survived the initial threshold were temporally and/or spatially clustered with neighboring bins that were also significant, and a cluster value was derived by summing all of the *t*-values of all of the data points in the cluster. Nonparametric permutation testing was then used to derive a distribution of cluster values and the significance level of the observed clusters was tested directly using this distribution. Based on this analysis, the time-frequency windows that contained significant oscillatory events across all participants were subjected to beamforming analyses. Further details of this method and our processing pipeline can be found in recent papers (Wiesman et al. 2017; Kurz et al. 2018; Spooner et al. 2018; Spooner, Eastman, et al. 2019; Spooner, Wiesman, et al. 2019; Arif, Spooner, et al. 2020; Arif, Wiesman, et al. 2020).

MEG Source Imaging

Cortical oscillatory networks were imaged through the dynamic imaging of coherent sources (DICS) beamformer (Gross et al. 2001), which uses the cross-spectral density matrices to calculate source power for the entire brain volume. These images are typically referred to as pseudo-*t* maps, with units (pseudo-*t*) that reflect noise-normalized power differences (i.e., active vs. passive) per voxel. Following convention, we computed noise-normalized, source power per voxel in each participant using baseline periods of equal duration and bandwidth (Hillebrand et al. 2005). MEG preprocessing and imaging used the (version 7.0; BESA) software.

Normalized source power was computed over the entire brain volume per participant at 4.0 × 4.0 × 4.0 mm resolution for the time-frequency periods identified through the sensor level analyses. Prior to statistical analysis, each participant's MEG data, which were coregistered to native space structural MRI prior to beamforming, were transformed into standardized space using the transform previously applied to the structural MRI volume and spatially resampled. The resulting 3D maps of brain activity were averaged across all participants and task conditions to assess the neuroanatomical basis of the significant oscillatory responses identified through the sensor-level analysis, and to allow identification of the peak voxels per oscillatory response.

Voxel time series data (i.e., "virtual sensors") were extracted from each participant's data individually using the peak voxel from the grand-averaged beamformer images. To compute the virtual sensors, we applied the sensor weighting matrix derived through the forward computation to the preprocessed signal vector, which yielded a time series for the specific coordinate in source space. Note that virtual sensor extraction was done per participant, once the coordinates of interest were known. Once the virtual sensor time series were extracted, we computed the envelope of the spectral power within the frequency range used in the beamforming analysis. From this time series, we computed the relative (i.e., baseline-corrected) response time series of each participant to quantify indices of movement-related oscillatory responses.

Statistical Analyses

To evaluate the influence of motor cortical dynamics on the age-related increases in susceptibility to response interference, we conducted multiple moderation analyses in R (*glm* package) for congruent and incongruent trials, separately, following standard data trimming procedures. Briefly, values exceeding 2.5 standard deviations from the group mean were considered outliers and excluded from subsequent data analyses. Specifically, we extracted perimovement virtual sensors from peak voxels in the contralateral (for theta and gamma) and bilateral (for alpha and beta) M1 for each frequency band specified in our beamformer analysis. Of note, because we did not have any hypotheses regarding hemispheric differences in the current study, bilateral recruitment of alpha and beta oscillatory responses were averaged across hemisphere for subsequent analyses. For congruent trials, the model included relative perimovement theta, alpha, beta, and gamma oscillatory power derived from congruent trials, as well as age as continuous predictors of congruent reaction time. In addition, moderators for each oscillatory response and age were computed (e.g., gamma power x age interaction) and included as continuous predictors of congruent reaction time. Importantly, to evaluate brain-behavior relationships during the processing of incongruent trials, the same moderation model was conducted—only now using virtual sensor data for each oscillatory response during incongruent trials, age, and their respective age by oscillatory-frequency interaction to predict incongruent reaction time. Finally, model comparisons between congruent and incongruent moderation models were performed using Fisher-Z transformations of each effect exhibiting significant associations in the overall models to evaluate differences in the predictive capacities of each effect as a function of task condition (Clogg et al. 1995; Paternoster et al. 1998). All reported *P*-values for pairwise comparisons survive stringent Bonferroni correction for multiple comparisons.

Results

Of the 69 participants who completed the current study and were not cognitively impaired, three were excluded due to excessive artifacts in their MEG data. The remaining 66 participants ($M_{age} = 44.9$, SD = 15.1, 32 females) were included in the final analyses.

Behavioral Performance

Participants performed well on the arrow-based Flanker task with an average reaction time of 656.71 ms (SD = 140.57 ms)

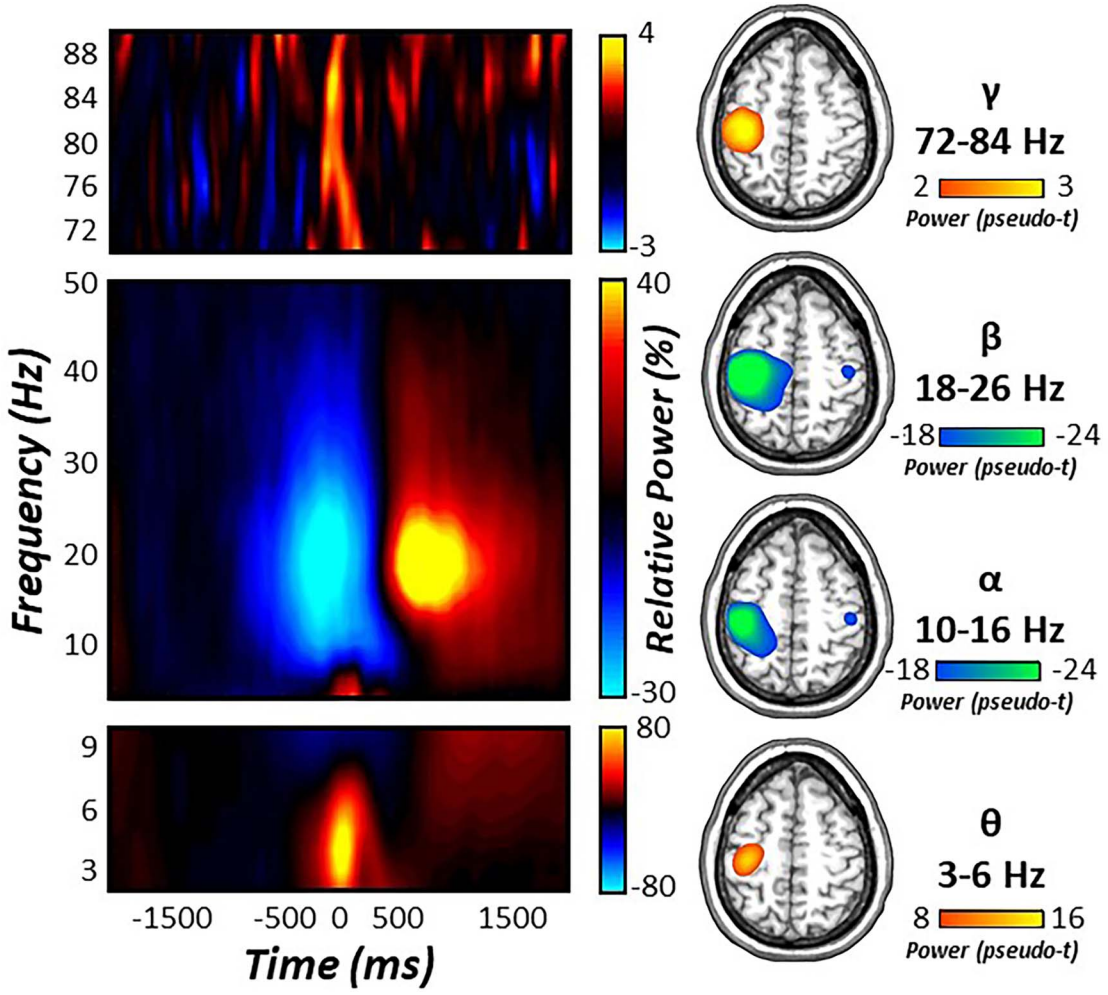

Figure 2. Sensor- and source-level neural responses during movement. (Left) Time-frequency spectrograms for three sensors near the contralateral sensorimotor cortex. The *x*-axis denotes time (in ms) and the *y*-axis denotes frequency (in Hz). Relative power is expressed as percent change from baseline (−1800 to −1000 ms) in the color scale bar to the right of each graphic. (Right) Significant movement-locked oscillatory responses were imaged using a beamformer and grand averaged across task conditions. Strong increases in theta (4–8 Hz) and gamma (72–84 Hz) activity were seen at movement onset in the left primary motor cortex. In contrast, strong decreases in alpha (10–16 Hz) and beta (18–26 Hz) activity were more temporally sustained prior to and following movement execution in the contralateral and ipsilateral primary motor cortices.

and mean accuracy of 97.94% (SD = 4.17%) across all trials. As expected, pairwise comparisons of task condition revealed a significant reaction time interference effect $t(66) = -8.32$, $P < 0.001$, such that participants were slower to respond to incongruent trials ($M = 685.06$ ms, SD = 149.48 ms) compared with congruent ones ($M = 628.35$ ms, SD = 136.87 ms; Fig. 1). In addition, chronological age was significantly predictive of this reaction time interference effect, $R(64) = 0.41$, $P = 0.001$, such that older adults exhibited larger behavioral decrements (i.e., slower reaction time) between congruent and incongruent conditions (Fig. 1).

Movement-Related Oscillations at the Sensor- and Source-Level

Statistical analysis of movement-locked time-frequency spectrograms revealed significant perimovement oscillatory responses in the theta (4–8 Hz), alpha (10–16 Hz), beta (18–26 Hz), and gamma (72–84 Hz) ranges. These responses were robust in sensors near the sensorimotor strip across all participants and both task conditions ($P < 0.001$, Fig. 2). Specifically, short-lived increases in low (i.e., theta) and high (i.e., gamma) frequencies were observed during movement onset (theta: −75 to 175 ms; gamma: −75 to 75 ms), while more temporally extended decreases in alpha and beta activity were observed prior to and following movement onset (alpha: −400 to 300 ms; beta: −400 to 200 ms). Importantly, since the goal of the study was to identify the possible role of motor control dynamics in the age-related decline in selective attention function, we did not further examine the prominent PMBR (Fig. 2), as it emerged after the termination of the motor response and, thereby, after the impact of the visual interference.

To identify the neural origins of oscillatory responses observed at the sensor-level, these time-frequency windows were imaged using a beamformer. The resulting maps were grand-averaged across all participants and experimental conditions. Interestingly, robust increases in theta and gamma oscillatory responses were observed in the left M1 cortices

(contralateral to movement), while strong decreases in alpha and beta activity were observed bilaterally in M1. As described in the methods, we next extracted virtual sensor time series from each respective grand-averaged cluster in the contralateral (i.e., for theta and gamma) and ipsilateral (i.e., for alpha and beta) M1 for congruent and incongruent trials separately to examine the effect of healthy aging on movement-related oscillations and subsequent behavioral performance.

Oscillatory Signatures of Movement Differentially Predict Response Interference in Healthy Aging

To evaluate the contribution of motor cortical oscillations in the age-related decline in selective attention performance, we conducted a multiple moderation analysis in R (*glm* package) for congruent and incongruent trials, separately. As described in the methods, our model consisted of perimovement theta, alpha, beta, and gamma oscillations during congruent trials and age defined as continuous predictors of congruent reaction time (Fig. 3). In addition, interaction terms of each movement-related oscillatory response and participant age were computed and included as continuous moderators of congruent reaction time. Interestingly, there was only a significant main effect of gamma oscillatory power on reaction time, such that increases in MRGS power in the contralateral M1 during congruent trials were predictive of faster congruent reaction times above and beyond all other motor cortical oscillations and participant age ($b = -1.59$, $P = 0.047$; Fig. 4). Similarly, using the same model for incongruent trials, there was a main effect of MRGS power on reaction time, such that increases in M1 gamma were predictive of faster incongruent reaction times above and beyond all other oscillatory signatures of movement and participant age ($b = -1.71$, $P = 0.012$; Fig. 4). In addition, we observed a significant MRGS power by age interaction, such that in younger adults, greater gamma power in the contralateral M1 during movement led to faster reaction times on incongruent trials, while older adults were unable to utilize this same resource in the contralateral M1 to support better behavioral performance ($b = 3.75$, $P = 0.007$; Fig. 5). For full model results, see Table 1.

Finally, we conducted model comparisons using Fisher-Z transformations of regression coefficients exhibiting significant associations in either model (i.e., gamma and gamma by age interaction) to evaluate the difference in predictive capacities of motor cortical oscillations on reaction time as a function of task condition. Interestingly, we found that the predictive capacity of the MRGS power by age interaction was stronger for incongruent reaction times compared with congruent ones ($Z = 2.52$, $P_{corr} = 0.012$), such that greater gamma power in the contralateral M1 during movement onset was predictive of faster reaction times in younger adults, and this effect was accentuated for incongruent compared with congruent trials (Fig. 5). In contrast, greater M1 gamma power was not associated with better behavioral performance in older adults for either task condition and further, this dissociation between younger and older adults was most apparent in the presence of response interference (i.e., during incongruent trials).

Discussion

The current study used advanced time series analyses of movement-related oscillatory activity to evaluate the contribution of the motor system to the well-established age-related declines found in selective attention function as measured by the Eriksen flanker task. Specifically, we found that perimovement increases in gamma activity (i.e., MRGS) in the contralateral M1 cortex robustly modulated behavior (i.e., faster reaction times) regardless of visual interference condition. However, the predictive capacity of high (i.e., gamma) frequency oscillations serving behavioral performance was greater in the presence of interference (i.e., incongruent trials), as evidenced by model comparisons of regression coefficients. In addition, age-related alterations in the MRGS response were differentially predictive of reaction times in the presence versus absence of distracting information. Importantly, our results suggest that the strength of the MRGS uniquely contributes to the well-known, age-related declines in selective attention performance, above and beyond other motor-related oscillations and chronological age alone. The implications of these novel findings are discussed below.

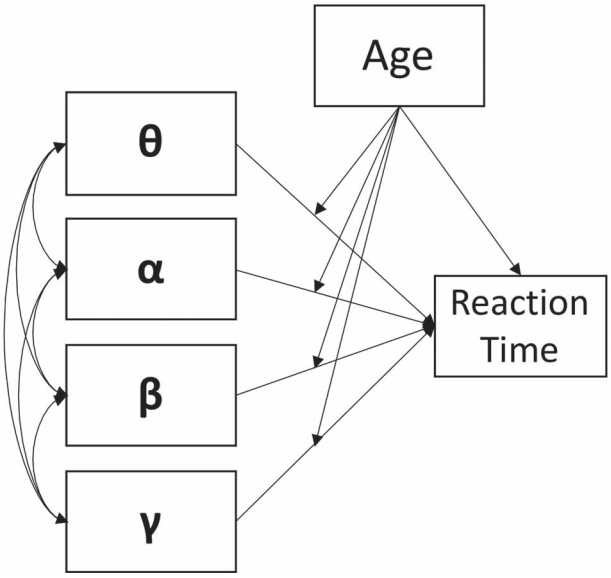

Figure 3. The conceptual multiple moderation model tested. Age is treated as a continuous moderator of the relationship between perimovement oscillatory power (i.e., theta, alpha, beta, and gamma) and participant reaction time for congruent and incongruent trials, separately.

Our findings suggesting that the strength of the MRGS predicts behavioral performance in the presence and absence of distracting information is not surprising, as previous studies have established this relationship during instances of response interference. For example, a previous study by Gaetz et al. (2013) found an earlier onset of MRGS responses during incongruent compared with congruent trials on a multisource interference task, which ultimately led to greater increases in gamma power prior to movement onset in the contralateral M1 and right inferior frontal gyrus (Gaetz et al. 2013). In a study using a modified Eriksen flanker task, investigators observed a similar trajectory in midfrontal areas prior to movement, such that gamma oscillatory activity occurred earlier and was increased in the presence of distracting stimuli; further, greater gamma activity at the sensor level was also related to greater behavioral costs following incongruent trials (Grent-'t-Jong et al. 2013). In a more recent study, Heinrichs-Graham et al. (2018) found significant alterations in movement-related peak gamma frequency in the contralateral M1 during the response itself, such that increases in peak gamma frequency were observed during

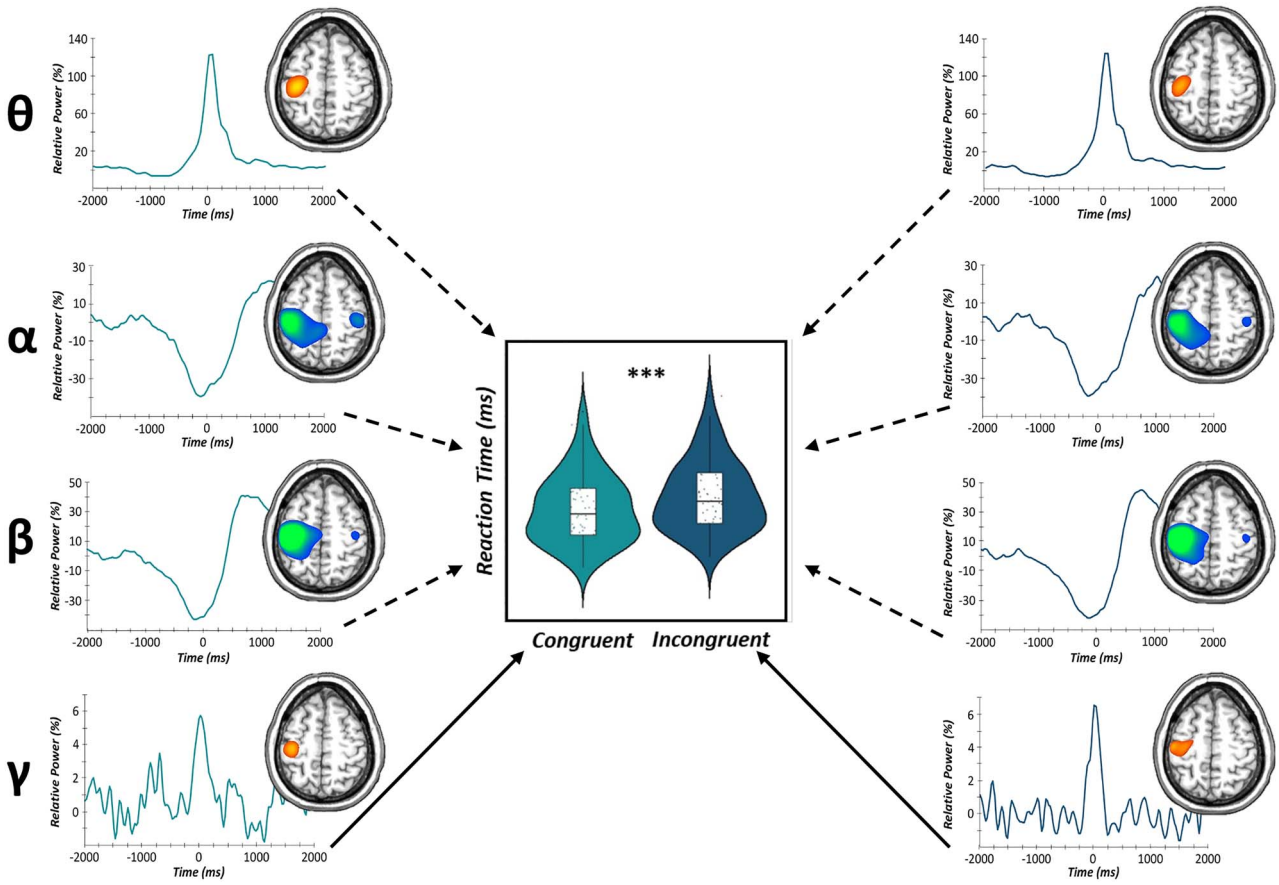

Figure 4. Movement-related gamma oscillations predict behavioral performance. Summary of the main effects of our multilevel moderation analyses of movement-related oscillatory power predicting reaction time for congruent (light blue) and incongruent (dark blue) trials, separately. (Left) Congruent trial virtual sensor data extracted from the grand-averaged peak voxels for each frequency band (top to bottom: theta, alpha, beta, gamma) differentially predicted congruent reaction time (in ms). Stronger MRGS responses during congruent trials were significantly predictive of faster congruent reaction times ($P = 0.047$). (Right) Incongruent virtual sensor data extracted for each perimovement frequency band (top to bottom: theta, alpha, beta, gamma). Stronger MRGS responses during incongruent trials were predictive of faster incongruent reaction times across all participants ($P = 0.012$). Solid lines denote significant predictive paths, while dashed lines are nonsignificant predictive paths. $^{***}P < 0.001$.

increased interference (Heinrichs-Graham et al. 2018). Similarly, Wiesman et al. (2020) found that increases in MRGS power in the premotor cortex contralateral to movement were sensitive to multiple sources of interference when presented simultaneously (Wiesman et al. 2020). Taken together, these studies align well with the current findings, which suggest that the spectral composition of movement-related gamma oscillations is sensitive to and predictive of behavioral performance during instances of increased interference. However, our results significantly extend these findings by showing that increases in gamma power in the contralateral M1 during the response itself is predictive of *better* performance on the selective attention task regardless of interference level and, importantly, above and beyond other oscillatory responses important for motor control. Critically, comparison with previous work in which the premovement gamma power/latency (e.g., −600 to −300 ms) changes led to worse task performance should be carefully considered (Gaetz et al. 2013; Grent-'t-Jong et al. 2013), as such modulation of behavior could be reflective of reaction time differences on the task. Essentially, stimulus onset would have occurred earlier during the interference trials, perhaps indicative of prolonged stimulus processing during interference conditions, rather than changes in the motor dynamics themselves.

Our most important finding was likely the modulation of MRGS by age and its differential behavioral performance predictive capacity as a function of response interference. Specifically, we observed a robust gamma power by age interaction on reaction time during instances of visual interference (i.e., incongruent trials), such that in younger adults, increases in MRGS power in the contralateral M1 were predictive of faster reaction times. However, older adults did not seem to utilize this same resource, such that during incongruent trials relative to congruent ones, the differential modulation of behavior with increasing age was attenuated. These results align nicely with a well-studied phenomenon in the field of cognitive aging known as the compensation-related utilization of neural resources hypothesis (CRUNCH; Reuter-Lorenz and Cappell 2008), which expands on traditional age-related compensation theories to index differences as a function of increasing cognitive loads. Essentially, this hypothesis suggests that older adults use disparate neural mechanisms compared with their younger counterparts in instances of lower and higher cognitive demand to achieve task goals. For example, in times of lower cognitive demand (e.g., reduced working memory load), older adults may engage larger volumes of tissue, recruit homologous brain regions, or increase the degree of activation to match the task

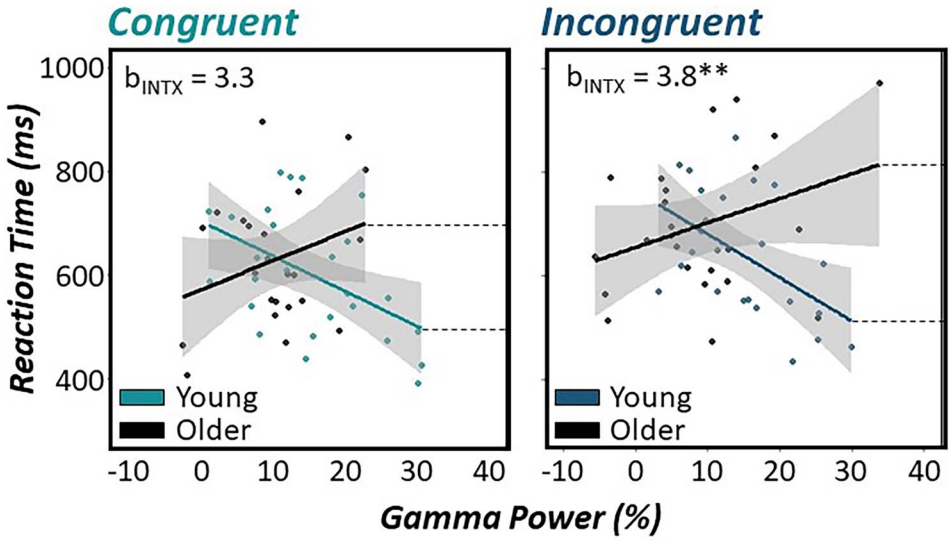

Figure 5. Age-related modulation of gamma activity in M1 differentially predicts response interference performance. Fisher-Z model comparisons revealed significantly different age by gamma interactions on reaction time between congruent and incongruent trials ($Z = 2.52$, $P_{corr} = 0.012$). Scatterplots denote the relationship between relative gamma power (%) on the *x*-axis and reaction time (in ms) on the *y*-axis. Regression lines depicting relationships for younger and older participants are based on ±0.5 SD cutoffs of the mean chronological age for each graph. These cutoffs were used for visualization purposes only, as chronological age was treated as a continuous variable in each model. 95% confidence intervals are shown in gray for each regression line. Estimated regression coefficients for the age by gamma interaction term are inset in the top left of each graph. For incongruent trials (right), there was a significant age by gamma interaction, such that in younger adults stronger MRGS responses were predictive of faster reaction times during incongruent trials, while the same relationship was not present in older adults. In contrast, this age by gamma interaction was not present for congruent trials (left). $^{**}P < 0.01$.

Table 1 Results of the multiple moderation analyses for congruent and incongruent trial data. (Top) Regression table of each oscillatory response, age and their interaction on congruent trial reaction time and incongruent trial reaction time (bottom). Significant effects are bolded for visibility. *p< .05.

Term	*b*	df	*t*	*P*-value	95% CI	
Congruent trial data						
Intercept	27.13	62	1.57	0.122	−6.66	60.92
Theta	0.01		0.11	0.916	−0.09	0.10
Theta x age	−0.10		−0.94	0.352	−0.29	0.10
Alpha	0.00		0.00	0.997	−1.09	1.09
Alpha x age	0.47		0.42	0.679	−1.76	2.70
Beta	−0.27		−0.40	0.694	−1.60	1.06
Beta x age	0.22		0.16	0.877	−2.56	3.00
Gamma	−1.60		−2.04	**0.047***	−3.13	−0.06
Gamma x age	3.30		1.87	0.067	−0.16	6.76
Age	−50.02		−1.25	0.216	−128.29	28.24
Incongruent trial data						
Intercept	26.00	61	1.50	0.139	−7.91	59.91
Theta	−0.03		−0.54	0.593	−0.13	0.07
Theta x age	−0.04		−0.36	0.722	−0.24	0.17
Alpha	0.08		0.18	0.862	−0.81	0.97
Alpha x age	0.35		0.37	0.714	−1.51	2.20
Beta	−0.55		−0.80	0.426	−1.89	0.79
Beta x age	0.95		0.69	0.496	−1.77	3.67
Gamma	−1.71		−2.60	**0.012***	−3.01	−0.42
Gamma x age	3.76		2.81	**0.007***	1.14	6.38
Age	−47.84		−1.34	0.185	−117.66	21.98

performance of younger adults (Reuter-Lorenz and Cappell 2008; Schneider-Garces et al. 2010). Alternatively, during times of higher cognitive demand (e.g., increased working memory load), this increased recruitment strategy becomes exhausted leading to poorer task performance. Importantly, this overactivation of neural resources is only considered compensatory when it is accompanied by age-invariant task performance in younger and older counterparts. In contrast, increased neural recruitment concomitant with behavioral decline is likely attributable to neural systems that have since lost specificity and/or selectivity

for carrying out task demands (i.e., dedifferentiation). While numerous studies using functional neuroimaging techniques (e.g., functional magnetic resonance imaging, positron emission tomography) have illuminated the neuroanatomical bases for dedifferentiation or neural inefficiency serving age-related cognitive dysfunction (Rypma et al. 2002, 2005, 2007; Zarahn et al. 2007; Reuter-Lorenz and Cappell 2008; Schneider-Garces et al. 2010), only recently have studies highlighted the contribution of spatially- and spectrally-distinct neuronal dynamics in these processes (Arif, Spooner, et al. 2020; Spooner, Wiesman, O'Neill, et al. 2020). For example, a recent study by Arif et al., used a modified Posner paradigm during MEG and found preferential engagement of alpha and beta oscillatory activity during attentional reorientation trials in frontoparietal hubs of younger adults, while this pattern was depleted in their older counterparts concomitant with age-related behavioral decrements during instances of increased task demands (i.e., attentional reorienting; Arif, Spooner, et al. 2020). In a latter study, Spooner and colleagues evaluated alterations in basic sensory processing in an aging sample of cognitively impaired and unimpaired HIV-infected adults and uninfected controls. Interestingly, they observed that younger cognitively impaired adults with HIV exhibited strong gamma oscillatory activity in prefrontal regions to filter repetitive somatosensory input. Importantly, this utilization of prefrontal resources during basic somatosensory processing effectively distinguished those with and without cognitive impairment and further, was diminished with advancing age in impaired adults with HIV (Spooner, Wiesman, O'Neill, et al. 2020). Taken together, these studies suggest that both the neuroanatomical *and* spectral properties of neuronal responses in older adults provides unique insight regarding the efficiency of aging neural systems and subsequent behavioral performance. Thus, we propose that the age-moderated changes in MRGS governing different levels of task performance, as observed in the current study, may be the result of exhausted neural resources with increasing age in the sensorimotor network, as we observed that in instances of higher cognitive demand (i.e., visual interference trials) stronger MRGS in the contralateral M1 did not yield better behavioral performance as it did in younger counterparts.

Mechanistically, the interference-related alterations in gamma oscillatory power and subsequent behavioral performance by age could be attributable at least in part to changes in intracortical inhibition. Notably, several electrophysiological studies suggest that the generation and modulation of pyramidal synchrony, including those at higher frequencies (i.e., gamma range: >30 Hz) is tightly linked to local GABA-mediated inhibitory drive (Bartos et al. 2007; Fries et al. 2007; Fries 2009, 2015; Buzsáki and Wang 2012; Vinck et al. 2013; Salkoff et al. 2015; Johnson et al. 2017). This work has been further corroborated by recent studies of human neuroimaging, which broadly suggest that spectral profiles of gamma activity in primary sensory cortices, including the motor cortex are related to local GABA concentrations (Edden et al. 2009; Muthukumaraswamy et al. 2009; Gaetz et al. 2011). For example, using GABA magnetic resonance spectroscopy, Gaetz et al. (2011) found that greater GABA concentrations in the M1 contralateral to movement were related to increases in peak MRGS frequency (Gaetz et al. 2011). In addition, studies of the visual system reported similar relationships within the primary visual cortices, such that elevations in peak gamma frequency and GABA concentration were related to better behavioral performance on an orientation discrimination task (Edden et al. 2009; Muthukumaraswamy et al. 2009). This speculation that GABAergic inhibitory drive may be contributing to our gamma-mediated brain/behavior relationships is further supported when considering the modulation of GABA *and* gamma profiles in the context of healthy aging (Gao et al. 2013). Critically, these studies demonstrate a robust relationship between decreases in both GABA concentration *and* MRGS frequency with increasing age in primary sensory and frontoparietal regions (Gaetz et al. 2011; Gao et al. 2013). *En masse*, these studies demonstrate that gamma oscillatory activity is critically dependent on local GABAergic intracortical inhibition and further, is modulated by the healthy aging process. While the evaluation of GABA was not a focus of the current study, perhaps our specific changes in MRGS power governing response interference may be the result of GABAergic dysfunction at the cellular level in aging populations. However, future studies are direly needed to fully unravel this relationship.

To conclude, this study was the first to establish the contribution of motor cortical oscillations to the age-related decline observed in selective attention performance. Specifically, we observed frequency-specific modulations of reaction time regardless of visual interference that were limited to the gamma band during the movement itself. In addition, we observed that condition-wise changes in the predictive capacity of motor-related oscillations and age on behavioral performance were limited to high frequency oscillations in the gamma range. Finally, a significant MRGS power by age interaction was observed during the processing of incongruent trials, but not congruent ones, such that younger adults who had stronger levels of gamma power in the contralateral M1 had faster reaction times. In contrast, older adults who had stronger MRGS within M1 did not receive the same behavioral benefit (i.e., faster reaction times) during times of higher cognitive demand, perhaps reflecting the exhaustion of neural resources with increasing age. In addition, we propose that this differential modulation of behavior in the presence of visual interference may be the result of local decreases in GABA concentration likely apparent in our aging sample, although direct relationships between intracortical inhibition and motor cortical oscillations during response interference must be established in future work to support this hypothesis. While the healthy aging process is known to involve a host of functional and behavioral changes as the result of altered neural dynamics during stimulus processing, the contribution of motor control dynamics to cognitive changes due to the presence of visual interference was far less understood. Importantly, these data were the first to suggest that gamma oscillatory activity within M1 may be sensitive to and predictive of the well-established decline in selective attention performance observed across the lifespan.

Funding

National Institutes of Health (NIH) grants R01-MH116782 to T.W.W., R01-MH118013 to T.W.W., R01-DA047828 to T.W.W., RF1-MH117032 to T.W.W., and T32-NS105594 to R.K.S.; National Science Foundation grant #1539067 to T.W.W.; NASA Nebraska Space Grant Fellowship (R.K.S.).

Notes

We would like to thank all of our volunteers for participating in the study, as well as our staff and collaborators for their

contributions. *Conflict of Interest*: The authors have no financial, commercial or institutional conflicts of interest to declare.

Data Availability Statement

Data from this study will be made available to qualified investigators upon reasonable request to the corresponding author.

References

Arif Y, Spooner RK, Wiesman AI, Embury CM, Proskovec AL, Wilson TW. 2020. Modulation of attention networks serving reorientation in healthy aging. *Aging (Albany NY)*. 12:12582–12597.

Arif Y, Wiesman AI, O'Neill J, Embury C, May PE, Lew BJ, Schantell MD, Fox HS, Swindells S, Wilson TW. 2020. The age-related trajectory of visual attention neural function is altered in adults living with HIV: a cross-sectional MEG study. *EBioMedicine*. 61:103065. [Epub ahead of print].

Aschenbrenner AJ, Balota DA. 2017. Dynamic adjustments of attentional control in healthy aging. *Psychol Aging*. 32:1–15.

Bartos M, Vida I, Jonas P. 2007. Synaptic mechanisms of synchronized gamma oscillations in inhibitory interneuron networks. *Nat Rev Neurosci*. 8:45–56.

Benedict R, Schretlen D, Groninger L, Brandt J. 1998. Hopkins verbal learning test-revised: normative data and analysis of inter-form and test-retest reliability. *Clin Neuropsychol*. 12:11.

Buzsáki G, Wang XJ. 2012. Mechanisms of gamma oscillations. *Annu Rev Neurosci*. 35:203–225.

Carrasco M. 2011. Visual attention: the past 25 years. *Vision Res*. 51:1484–1525.

Cassim F, Monaca C, Szurhaj W, Bourriez JL, Defebvre L, Derambure P, Guieu JD. 2001. Does post-movement beta synchronization reflect an idling motor cortex? *Neuroreport*. 12:3859–3863.

Cheyne D, Bells S, Ferrari P, Gaetz W, Bostan AC. 2008. Self-paced movements induce high-frequency gamma oscillations in primary motor cortex. *Neuroimage*. 42:332–342.

Cheyne D, Ferrari P. 2013. MEG studies of motor cortex gamma oscillations: evidence for a gamma "fingerprint" in the brain? *Front Hum Neurosci*. 7:575.

Clogg C, Petkova E, Haritou A. 1995. Statistical models comparing regression coefficients between models. *American Journal of Sociology*. 100:32.

Comalli PE, Wapner S, Werner H. 1962. Interference effects of Stroop color-word test in childhood, adulthood and aging. *J Genet Psychol*. 100:47–53.

Driver J. 2001. A selective review of selective attention research from the past century. *Br J Psychol. 92 Part*. 1:53–78.

Edden RA, Muthukumaraswamy SD, Freeman TC, Singh KD. 2009. Orientation discrimination performance is predicted by GABA concentration and gamma oscillation frequency in human primary visual cortex. *J Neurosci*. 29:15721–15726.

Fries P. 2009. Neuronal gamma-band synchronization as a fundamental process in cortical computation. *Annu Rev Neurosci*. 32:209–224.

Fries P. 2015. Rhythms for cognition: communication through coherence. *Neuron*. 88:220–235.

Fries P, Nikolić D, Singer W. 2007. The gamma cycle. *Trends Neurosci*. 30:309–316.

Gaetz W, Edgar JC, Wang DJ, Roberts TP. 2011. Relating MEG measured motor cortical oscillations to resting γ-aminobutyric acid (GABA) concentration. *Neuroimage*. 55:616–621.

Gaetz W, Liu C, Zhu H, Bloy L, Roberts TP. 2013. Evidence for a motor gamma-band network governing response interference. *Neuroimage*. 74:245–253.

Gaetz W, Macdonald M, Cheyne D, Snead OC. 2010. Neuromagnetic imaging of movement-related cortical oscillations in children and adults: age predicts post-movement beta rebound. *Neuroimage*. 51:792–807.

Gao F, Edden RA, Li M, Puts NA, Wang G, Liu C, Zhao B, Wang H, Bai X, Zhao C, et al. 2013. Edited magnetic resonance spectroscopy detects an age-related decline in brain GABA levels. *Neuroimage*. 78:75–82.

Geerligs L, Saliasi E, Maurits NM, Renken RJ, Lorist MM. 2014. Brain mechanisms underlying the effects of aging on different aspects of selective attention. *Neuroimage*. 91:52–62.

Grent-'t-Jong T, Oostenveld R, Jensen O, Medendorp WP, Praamstra P. 2013. Oscillatory dynamics of response competition in human sensorimotor cortex. *Neuroimage*. 83:27–34.

Grent-'t-Jong T, Oostenveld R, Jensen O, Medendorp WP, Praamstra P. 2014. Competitive interactions in sensorimotor cortex: oscillations express separation between alternative movement targets. *J Neurophysiol*. 112:224–232.

Gross J, Kujala J, Hamalainen M, Timmermann L, Schnitzler A, Salmelin R. 2001. Dynamic imaging of coherent sources: studying neural interactions in the human brain. *Proc Natl Acad Sci U S A*. 98:694–699.

Hämäläinen M, Hari R, Ilmoniemi RJ, Knuutila J, Lounasmaa OV. 1993. Magnetoencephalography—theory, instrumentation, and applications to noninvasive studies of the working human brain. *Rev Mod Phys*. 65:413–497.

Hasher L, Stoltzfus ER, Zacks RT, Rypma B. 1991. Age and inhibition. *J Exp Psychol Learn Mem Cogn*. 17:163–169.

Heaton R, Miller S, Taylor M, Grant I. 2004. *Revised comprehensive norms for an expanded Halstead-Reitan battery: demographically adjusted neuropsychological norms for African American and Caucasian adults*. Lutz, FL: Psychological Assessment Resources.

Heinrichs-Graham E, Arpin DJ, Wilson TW. 2016. Cue-related temporal factors modulate movement-related Beta oscillatory activity in the human motor circuit. *J Cogn Neurosci*. 28:1039–1051.

Heinrichs-Graham E, Hoburg JM, Wilson TW. 2018. The peak frequency of motor-related gamma oscillations is modulated by response competition. *Neuroimage*. 165:27–34.

Heinrichs-Graham E, Kurz MJ, Gehringer JE, Wilson TW. 2017. The functional role of post-movement beta oscillations in motor termination. *Brain Struct Funct*. 222:3075–3086.

Heinrichs-Graham E, Wilson TW. 2015. Coding complexity in the human motor circuit. *Hum Brain Mapp*. 36:5155–5167.

Hillebrand A, Singh KD, Holliday IE, Furlong PL, Barnes GR. 2005. A new approach to neuroimaging with magnetoencephalography. *Hum Brain Mapp*. 25:199–211.

Igarashi J, Isomura Y, Arai K, Harukuni R, Fukai T. 2013. A θ-γ oscillation code for neuronal coordination during motor behavior. *J Neurosci*. 33:18515–18530.

Jefferson AL, Paul RH, Ozonoff A, Cohen RA. 2006. Evaluating elements of executive functioning as predictors of instrumental activities of daily living (IADLs). *Arch Clin Neuropsychol*. 21:311–320.

Johnson NW, Özkan M, Burgess AP, Prokic EJ, Wafford KA, O'Neill MJ, Greenhill SD, Stanford IM, Woodhall GL. 2017. Phase-amplitude coupled persistent theta and gamma oscillations in rat primary motor cortex in vitro. *Neuropharmacology*. 119:141–156.

Jurkiewicz MT, Gaetz WC, Bostan AC, Cheyne D. 2006. Post-movement beta rebound is generated in motor cortex: evidence from neuromagnetic recordings. *Neuroimage*. 32:1281–1289.

Kawai N, Kubo-Kawai N, Kubo K, Terazawa T, Masataka N. 2012. Distinct aging effects for two types of inhibition in older adults: a near-infrared spectroscopy study on the Simon task and the flanker task. *Neuroreport*. 23:819–824.

Klove H. 1963. *Grooved pegboard*. Lafayette, IN: Lafayette Instruments.

Kovach CK, Gander PE. 2016. The demodulated band transform. *J Neurosci Methods*. 261:135–154.

Kurz MJ, Wiesman AI, Coolidge NM, Wilson TW. 2018. Children with cerebral palsy hyper-gate somatosensory stimulations of the foot. *Cereb Cortex*. 28:2431–2438.

Langner R, Cieslik EC, Behrwind SD, Roski C, Caspers S, Amunts K, Eickhoff SB. 2015. Aging and response conflict solution: behavioural and functional connectivity changes. *Brain Struct Funct*. 220:1739–1757.

Muthukumaraswamy SD. 2010. Functional properties of human primary motor cortex gamma oscillations. *J Neurophysiol*. 104:2873–2885.

Muthukumaraswamy SD, Edden RA, Jones DK, Swettenham JB, Singh KD. 2009. Resting GABA concentration predicts peak gamma frequency and fMRI amplitude in response to visual stimulation in humans. *Proc Natl Acad Sci U S A*. 106:8356–8361.

Paternoster R, Brame R, Mazerolle P, Piquero A. 1998. Using the correct statistical test for equality of regression coefficients. *Criminology* 36:7.

Pfurtscheller G, Lopes da Silva FH. 1999. Event-related EEG/MEG synchronization and desynchronization: basic principles. *Clin Neurophysiol*. 110:1842–1857.

Plude DJ, Doussard-Roosevelt JA. 1989. Aging, selective attention and feature integration. *Psychol Aging*. 4:98–105.

Reuter-Lorenz PA, Cappell KA. 2008. Neurocognitive aging and the compensation hypothesis. *Curr Dir Psychol Sci*. 17: 177–182.

Rypma B, Berger JS, D'Esposito M. 2002. The influence of working-memory demand and subject performance on prefrontal cortical activity. *J Cogn Neurosci*. 14:721–731.

Rypma B, Berger JS, Genova HM, Rebbechi D, D'Esposito M. 2005. Dissociating age-related changes in cognitive strategy and neural efficiency using event-related fMRI. *Cortex*. 41: 582–594.

Rypma B, Eldreth DA, Rebbechi D. 2007. Age-related differences in activation-performance relations in delayed-response tasks: a multiple component analysis. *Cortex*. 43:65–76.

Salkoff DB, Zagha E, Yüzgeç Ö, McCormick DA. 2015. Synaptic mechanisms of tight spike synchrony at gamma frequency in cerebral cortex. *J Neurosci*. 35:10236–10251.

Schneider-Garces NJ, Gordon BA, Brumback-Peltz CR, Shin E, Lee Y, Sutton BP, Maclin EL, Gratton G, Fabiani M. 2010. Span, CRUNCH, and beyond: working memory capacity and the aging brain. *J Cogn Neurosci*. 22:655–669.

Spooner RK, Eastman JA, Rezich MT, Wilson TW. 2019. High-definition transcranial direct current stimulation dissociates fronto-visual theta lateralization during visual selective attention. *J Physiol*. 598:987–998.

Spooner RK, Wiesman AI, Mills MS, O'Neill J, Robertson KR, Fox HS, Swindells S, Wilson TW. 2018. Aberrant oscillatory dynamics during somatosensory processing in HIV-infected adults. *Neuroimage Clin*. 20:85–91.

Spooner RK, Wiesman AI, O'Neill J, Schantell MD, Fox HS, Swindells S, Wilson TW. 2020. Prefrontal gating of sensory input differentiates cognitively impaired and unimpaired aging adults with HIV. *Brain Commun*. 2:fcaa080.

Spooner RK, Wiesman AI, Proskovec AL, Heinrichs-Graham E, Wilson TW. 2020. Prefrontal theta modulates sensorimotor gamma networks during the reorienting of attention. *Hum Brain Mapp*. 41:520–529.

Spooner RK, Wiesman AI, Proskovec AL, Heinrichs-Graham E, Wilson TW. 2019. Rhythmic spontaneous activity mediates the age-related decline in somatosensory function. *Cereb Cortex*. 29:680–688.

Taulu S, Simola J. 2006. Spatiotemporal signal space separation method for rejecting nearby interference in MEG measurements. *Phys Med Biol*. 51:1759–1768.

Tomassini A, Ambrogioni L, Medendorp WP, Maris E. 2017. Theta oscillations locked to intended actions rhythmically modulate perception. *Elife*. 6:e25618.

Tzagarakis C, Ince NF, Leuthold AC, Pellizzer G. 2010. Beta-band activity during motor planning reflects response uncertainty. *J Neurosci*. 30:11270–11277.

Uusitalo MA, Ilmoniemi RJ. 1997. Signal-space projection method for separating MEG or EEG into components. *Med Biol Eng Comput*. 35:135–140.

Vinck M, Womelsdorf T, Buffalo EA, Desimone R, Fries P. 2013. Attentional modulation of cell-class-specific gamma-band synchronization in awake monkey area v4. *Neuron*. 80:1077–1089.

Wechsler D. 1997. *Wechsler adult intelligence scale*. Third Edition. San Antonio, TX: Psychological Corporation.

Wiesman AI, Heinrichs-Graham E, Coolidge NM, Gehringer JE, Kurz MJ, Wilson TW. 2017. Oscillatory dynamics and functional connectivity during gating of primary somatosensory responses. *J Physiol*. 595:1365–1375.

Wiesman AI, Koshy SM, Heinrichs-Graham E, Wilson TW. 2020. Beta and gamma oscillations index cognitive interference effects across a distributed motor network. *Neuroimage*. 116747. [Epub ahead of print].

Williams RS, Kudus F, Dyson BJ, Spaniol J. 2018. Transient and sustained incentive effects on electrophysiological indices of cognitive control in younger and older adults. *Cogn Affect Behav Neurosci*. 18:313–330.

Wilson TW, Fleischer A, Archer D, Hayasaka S, Sawaki L. 2011. Oscillatory MEG motor activity reflects therapy-related plasticity in stroke patients. *Neurorehabil Neural Repair*. 25(2):188–93.

Wilson TW, Heinrichs-Graham E, Becker KM. 2014. Circadian modulation of motor-related beta oscillatory responses. *Neuroimage*. 102(Pt 2):531–539.

Wilson TW, Heinrichs-Graham E, Proskovec AL, McDermott TJ. 2016. Neuroimaging with magnetoencephalography: a dynamic view of brain pathophysiology. *Transl Res*. 175:17–36.

Wilson TW, Slason E, Asherin R, Kronberg E, Reite ML, Teale PD, Rojas DC. 2010. An extended motor network generates beta and gamma oscillatory perturbations during development. *Brain Cogn*. 73:75–84.

Zarahn E, Rakitin B, Abela D, Flynn J, Stern Y. 2007. Age-related changes in brain activation during a delayed item recognition task. *Neurobiol Aging*. 28:784–798.